

# THE SCATTERING OF 1 MeV ELECTRONS AND POSITRONS

By J. A. McDONELL\*

[Manuscript received June 1, 1953]

## Summary

Electrons and positrons of energy 1 MeV were selected by a  $\beta$ -ray spectrometer and scattered by a gold foil. The scattered particles were detected by a coincidence Geiger counter arrangement, using the same geometry for electrons and positrons. The results show that the ratio of the fraction of electrons scattered through an angle  $\theta$  to the fraction of positrons scattered through  $\theta$  varies with  $\theta$ , and the magnitudes of the ratios agree with those predicted by theory. It is also inferred that there is a difference between the multiple scattering of electrons and positrons under the same scattering conditions.

## I. INTRODUCTION

Many investigations of the single elastic scattering of electrons have been carried out since Mott (1929) calculated the cross section for the process, using the Dirac wave equation for the electron. He showed that the probability that an electron will be scattered into an element of solid angle  $d\Omega$  at an angle  $\chi$  to its original direction is given by

$$I(\chi)d\Omega = \kappa^2 \cdot R(\chi) \operatorname{cosec}^4 \frac{1}{2}\chi \cdot d\Omega,$$

where

$$\kappa^2 = \left( \frac{Ze^2w}{2mc^2(w^2-1)} \right)^2 \frac{N\sigma}{M}.$$

$Z$ ,  $M$ , and  $\sigma$  are the atomic number, atomic weight, and surface density in  $\text{g cm}^{-2}$  of the scatterer, and  $e$ ,  $m$ , and  $w$  are the charge, mass, and total energy in  $mc^2$  units, of the electron.  $N$  is Avogadro's number.

$\kappa^2 \operatorname{cosec}^4 \frac{1}{2}\chi$  is the form of the cross section obtained from the relativistic Schrödinger equation, and is generally referred to as the "relativistic Rutherford" cross section. The important function is  $R(\chi)$ , which is dependent on  $\beta$  ( $=v/c$ ) and  $\alpha$  ( $=Z/137$ ), and arises from the presence in the Dirac equation of terms which take account of the spin of the electron. For small values of  $\alpha$ , values of  $R(\chi)$  can be calculated from the first approximation

$$R(\chi) = 1 - \beta^2 \sin^2 \frac{1}{2}\chi + \pi\alpha\beta \sin \frac{1}{2}\chi \cdot (1 - \sin \frac{1}{2}\chi).$$

For larger values of  $\alpha$ ,  $R(\chi)$  must be calculated numerically. Bartlett and Watson (1940) have performed the calculation for  $Z=80$  and energies up to 1.7 MeV, and McKinley and Feshbach (1948), using an approximation in which only terms of order  $\alpha^2$  are retained, have calculated  $R(\chi)$  for 1, 2, and 4 MeV and all values of  $Z$ . In both of these calculations, the interaction between the electron and the nucleus is represented by an unscreened Coulomb field.

\* Physics Department, University of Melbourne.

For an energy of 1 MeV, with which we will be concerned, the most reliable calculation using a screened atomic field is that of Gunnarsen (1952) for  $Z=80$ . His results show that the effect of screening is probably very small.

Massey (1942) calculated  $R(\chi)$  for positron scattering, his calculations being based on those of Bartlett and Watson, with  $Z$  changed to  $-Z$  throughout. He found that the values of  $R(\chi)$  for electrons and positrons were quite different, and pointed out that measurements of the ratio of electron intensity to positron intensity under identical scattering conditions (hereafter called the electron-positron ratio) would provide a much more sensitive test of the theory than measurements with electrons alone. Experiments of the latter type had, up till that time, given rather conflicting results.

More recently, accurate measurements using accelerated beams of electrons have shown good agreement with theory (Van de Graaff, Buechner, and Feshbach 1946; Buechner *et al.* 1947), but at the time when the present work was commenced, no satisfactory measurements of the electron-positron ratio had been made, although cloud-chamber measurements by Fowler and Oppenheimer (1938) and Lasich (1948) had suggested that the ratio was of the order predicted by theory. Since then Lipkin (1952) has made accurate measurements of scattering at an angle of  $58^\circ$  using platinum and copper foils as scatterers and particles having various energies in the region of 1 MeV. The values of the electron-positron ratio which he obtains are generally 10 per cent. larger than the theoretical values. Howatson and Atkinson (1951) have observed the scattering of electrons and positrons by argon in a cloud chamber, and find good agreement with theory for the total number of scatters through angles greater than  $20^\circ$ . However, because of the small number of events involved (70 electrons and 66 positrons), their observations do not permit a significant estimate of the electron-positron ratio as a function of the scattering angle. Cusack (1952), in a similar experiment, but using positrons only, and nitrogen as the scatterer, obtained 114 scatters through angles greater than  $20^\circ$ . The expected number was 181, and he was unable to account for this discrepancy.

The present experiment was designed to measure the electron-positron ratio at various angles for 1.07 MeV particles scattered in gold. This energy was used by Gunnarsen in his calculations.

## II. APPARATUS

### (a) *The Spectrometer*

A short magnetic lens  $\beta$ -ray spectrometer was constructed to provide particles having energies within a small range. The instrument was similar to that of Deutsch, Elliott, and Evans (1944), and their calculations of trajectories were used in its design. From the description of the scattering arrangement which follows, it will be seen that it was desirable to focus the beam within as small an area as possible. Since the sources could not conveniently be deposited within a circle of less than  $\frac{1}{4}$  in. diameter, a magnification greater than one would not have been satisfactory. On the other hand, as the magnification is

decreased, so is the transmission of the instrument, and hence the intensity of the available beam. Therefore the instrument was adjusted for unit magnification, with the central aperture fairly wide, thereby reducing the resolution in an endeavour to increase the transmission. The resolution, as measured by the width of the transmission curve at half-maximum, was 7 per cent.

During a preliminary run, it was found that particles scattered from the edges of the  $\frac{1}{4}$  in. diameter exit window which ultimately defined the focused beam, were making a significant contribution to the measured count rates. This window was then machined to a diameter of  $1\frac{1}{2}$  in., and other defining baffles introduced further back in the spectrometer. In this way the image of the source was confined almost entirely to a circle of  $\frac{1}{4}$  in. diameter centred on the axis of the spectrometer, and in a plane  $\frac{1}{2}$  in. beyond this last  $1\frac{1}{2}$  in. diameter aperture. The size of the image and its location (determined by the final lining-up of the spectrometer) were examined by the use of the photographic film.

#### (b) *The Scattering Arrangement*

The arrangement of the scattering foil and the detector for the scattered particles is shown in Figure 1. The gold foil was prepared by plating gold on a thin polished copper foil, and then removing the copper with nitric acid. The foil was then mounted over one of two  $\frac{7}{8}$  in. diameter holes on a vane which could be rotated by a shaft through an O-ring seal. The other hole was left blank. The foil was mounted on the side of the vane furthest from the source, and the plane of this face contained the focused image. Thus, the beam of particles could be made to pass either through the centre of the scatterer or through the centre of the blank hole. It was found that the centering of the foil or the blank hole on the spectrometer axis was best achieved by installing a small light globe inside the vacuum system, and observing the rotation of the vane visually through a piece of plate glass waxed over a small hole in the centre of the end wall of the vacuum chamber.

The scattered particles were detected by a counter whose axis was horizontal and passed through the centre of the image. This counter was mounted so that it could be rotated about a vertical axis, also through the centre of the image, the rotation being effected by an O-ring seal. A pointer rotating with the counter but outside the vacuum system moved across an angular scale, and provided a measure of  $\theta$ , the angle which the counter axis made with the spectrometer axis, to within  $\pm 1^\circ$ .

In the design of the counter, the main consideration was reduction of the high background produced by the energetic  $\gamma$ -rays from the positron source. It was found that these were strongly scattered in the magnet coil of the spectrometer, producing a high  $\gamma$ -ray flux in the region of the detector. This was no doubt increased by a certain amount of annihilation radiation from positrons striking the baffles in the spectrometer.

Accordingly, a counter had to be designed having a high directional sensitivity. The form finally chosen is shown in Figure 2. The counter is of the Maze type, with a body of high conductivity soda glass, and an external

"Aquadag" cathode. The cathode is "split" into three sections, and the centre section is at the anode potential, so that a discharge at one end of the

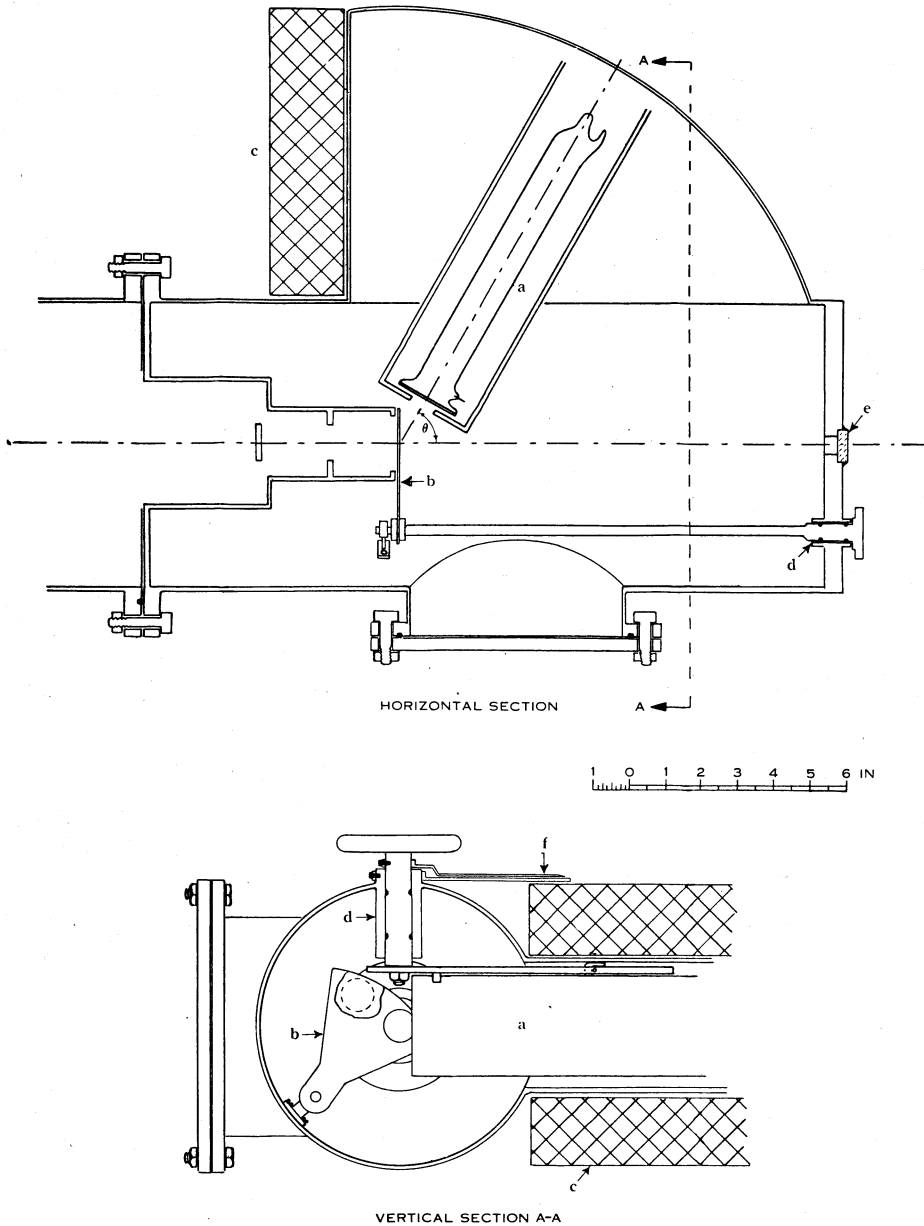


Fig. 1.—Scattering arrangement. *a*, Counter in brass box ; *b*, vane carrying gold foil ; *c*, lead shielding ; *d*, O-ring seals ; *e*, glass window ; *f*, pointer and angular scale.

counter cannot travel to the other end. Positive pulses are taken off each of the two outside cathode sections, and coincidences between them counted. Thus a

single particle is counted only when it traverses practically the whole counter, and its path makes only a fairly small angle with the counter axis. As an indication of the effectiveness of this arrangement, its cosmic ray background with the axis horizontal was 0.5/min. The conductivity of the soda glass was high enough to prevent any appreciable decrease in pulse height as the count rate increased. To reduce further the  $\gamma$ -ray background, the quadrant in which the counter rotated (Fig. 1) was lead-shielded above, below, and on the side nearest the magnet coil.

The end window of the counter was made of soda glass, sealed on to the body with solder glass. The window was thick enough to absorb electrons of energy less than 0.85 MeV, this energy limit being checked using the direct beam of focused electrons in the spectrometer. Thus any particles scattered inelastically through the angles at which measurements were taken would not be detected, nor would any "stray" low-energy particles such as were observed by Schulze-Pillot and Bothe (1950) in their spectrometer.

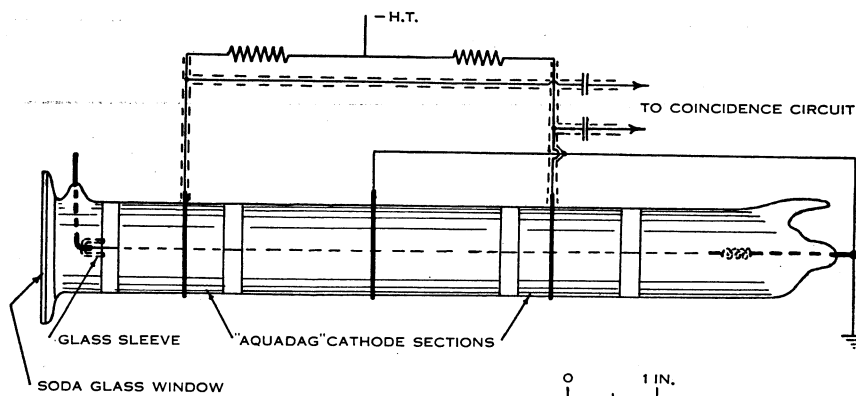


Fig. 2.—End window directional counter.

There is reason to expect that this absorber would affect identical beams of electrons and positrons rather differently. However, the relative strengths of the electron and positron beams incident on the scatterer were measured using this same counter, in the manner described below. Therefore, since the quantities which we measure have the form

$$\frac{\text{Fraction of incident electrons scattered through } \theta}{\text{Fraction of incident positrons scattered through } \theta'}$$

the presence of an absorber will not affect the results unless the energy distributions of the *scattered* electrons and positrons differ as a result of their having traversed the gold foil. There is no reason to believe that positrons differ greatly from electrons in the way they lose small amounts of energy, and since the theory of Landau (1944) gives the most probable energy loss for electrons in this case as 0.6 per cent. of the initial energy, one can assume that the effect of any such difference in our measurements is negligible.

## (c) Sources\*

The energy calibration of the spectrometer was obtained using the photo-electrons produced in Pb by the  $\gamma$ -rays of  $^{60}\text{Co}$ . The energies of these  $\gamma$ -rays have been accurately measured by Lind, Brown, and Du Mond (1949).

The sources of positrons and electrons had to be chosen subject to the fairly severe limitations of having a spectrum with maximum energy rather greater than 1 MeV, and a half-life of at least several days, since all radioactive materials had to be imported. Of the possible electron sources, the most readily available was  $^{32}\text{P}$  (obtained from Harwell) and a 20 mc source of this isotope was found to be quite satisfactory. A further advantage is that  $^{32}\text{P}$  has no  $\gamma$ -rays, and therefore the background count is at a minimum. For a positron source, however, there is no choice, as the only available positron emitter with suitable energy and half-life is  $^{56}\text{Co}$ . While this isotope has a maximum positron energy of 1.5 MeV and a half-life of 75 days, it has certain less desirable features from our point of view.

TABLE 1  
ISOTOPES PRESENT IN A SOURCE OF RADIO-COBALT

Isotope	$^{56}\text{Co}$	$^{57}\text{Co}$	$^{58}\text{Co}$
Half-life (days) .. ..	75	270	75
Decay particles	$\beta^+$ , 0.995	$\beta^+$ , 0.315	$\beta^+$ , 0.45
(max. energy MeV) ..	$\beta^+$ , 1.53		
$\gamma$ -Ray energies (MeV) ..	0.845	0.119	0.805
	1.26	0.131	
	1.74		
	2.01		
	2.55		
	3.25		
Production .. ..	$^{56}\text{Fe-d-2n}$	$^{56}\text{Fe-d-n}$	$^{57}\text{Fe-d-n}$

$^{56}\text{Co}$  is produced by deuteron bombardment of Fe or Ni, or by  $\alpha$ -particle bombardment of Mn, but in all cases, other cobalt isotopes are formed as well. The most recent investigation of these isotopes is that of Cheng, Dick, and Kurbatov (1952). In our case, the radio-cobalt was produced by deuteron bombardment of  $\text{Fe}^\dagger$ , and the main isotopes present are those shown in Table 1. After the conclusion of the scattering measurements, the  $\beta$ - and  $\gamma$ -spectra of the cobalt source were investigated. The spectra obtained were in good agreement with those previously reported.

Although no published data are available, one would assume that the Fe-d-n reaction would be more probable than the Fe-d-2n reaction, so that a

\* All radioactive materials used in this work were obtained through the agency of the Tracer Elements Section, C.S.I.R.O.

$\dagger$  We are very grateful to the Department of Terrestrial Magnetism, Washington, U.S.A., which prepared this source.

cobalt source of given strength would contain more  $^{57}\text{Co}$  than  $^{56}\text{Co}$ . Further, if the strength of the source is estimated from  $\gamma$ -ray intensity measurements, it is likely that the measured intensity will be largely due to the 119 keV and 131 keV  $\gamma$ -rays of  $^{57}\text{Co}$ . It is assumed that effects such as this account for the fact that the number of 1 MeV electrons from 20 mc of  $^{32}\text{P}$  was 160 times greater than the number of 1 MeV positrons from our 12 mc source of radio-cobalt. (These source strengths are those quoted by Harwell and the Department of Terrestrial Magnetism.)

### III. EXPERIMENTAL PROCEDURE

The surface density of the foil was measured as follows. A piece of foil (about  $5\text{ cm}^2$ ) from the same sample from which the scatterer was taken was placed on a piece of glass and illuminated from below. It was then covered by a piece of graph paper having millimetre divisions of good precision. The outline of the piece of foil was carefully traced on the graph paper and its area estimated by counting squares. The piece was then weighed. It was then divided in two and the procedure repeated for each small piece. The surface densities thus obtained were: for the whole piece,  $9.65\text{ mg cm}^{-2}$  and, for the two small pieces,  $9.65$  and  $9.67\text{ mg cm}^{-2}$ . On the basis of these measurements, the foil was taken to be sufficiently uniform, and of surface density  $9.65\text{ mg cm}^{-2}$ .

With the counter set at a particular angle, and the beam passing through the blank hole, the count rate was made up of contributions from:

- (a) cosmic radiation,
- (b)  $\gamma$ -ray background (for the positron source only),
- (c) electrons scattered into the counter from baffles etc. in the apparatus.

With the foil brought into position, the count rate was made up of (a) and (b), together with electrons scattered by the foil, and some fraction of (c). This fraction was unknown, unless one could in some way determine whether the source of these particles lay in front of, or behind the scatterer. Thus the baffles were located as described above in order to reduce (c) to negligible proportions. Under these conditions, the count rate due to electrons scattered by the foil is just the difference between the rates with the foil "in" and "out".

As a check on the effectiveness of the baffle arrangement, the count rate as a function of  $\theta$  with the foil out was measured before the scattering measurements were commenced, using a  $^{32}\text{P}$  source. Since this source emits no  $\gamma$ -rays, all electrons counted in this measurement must have been in category (c). The result is shown in Figure 3, and indicates that satisfactory measurements of the particles scattered from the foil could be expected for  $\theta \geq 40^\circ$ . The "plateau" at about  $10^\circ$  on the curve in Figure 3 is due to particles entering the counter from the direct beam of the spectrometer. The intensities of the positron and electron beams incident on the foil were compared by measuring the count rates at  $\theta = 10^\circ$ , with the foil out.

While measurements of the electron-positron ratio would not be affected by any variation with  $\theta$  of the effective solid angle subtended at the centre of the scatterer by the counter, measurements of the relative intensities at different

angles for electrons or positrons alone are of some interest. For such measurements, some information about this solid angle is necessary. A thin (less than  $0.1 \text{ mg cm}^{-2}$ ) "Formvar" film was temporarily mounted over the blank hole in the vane, and a small amount of  $^{32}\text{P}$  evaporated at its centre. This was then lined up on the spectrometer axis, providing a source of electrons isotropically

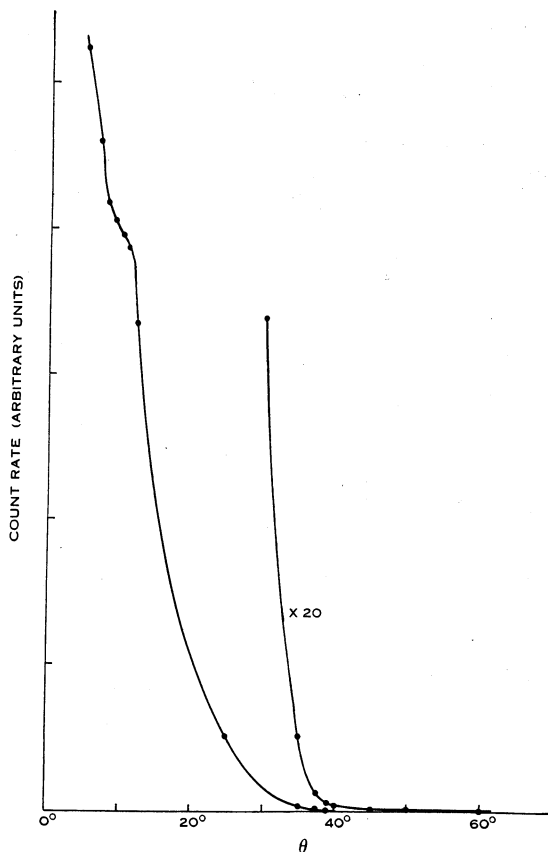


Fig. 3.—Count rate *v.* angle with foil out and  $^{32}\text{P}$  source.

distributed in space, except for directions making small angles with the plane of the film, where some effect due to backscattering might have been expected. The count rate under these conditions was constant for  $\theta \leq 70^\circ$ . Thus the angular range in which scattering measurements were made was  $40^\circ \leq \theta \leq 70^\circ$ .

For the scattering measurements using positrons, the following procedure was adopted. At the beginning of each day, a count was taken in the  $10^\circ$ , foil out position. This served to monitor the decay of the source, and also to check that the apparatus was operating correctly. Four-hour counts were then taken in the foil out and foil in positions for a certain angle, say  $70^\circ$ . On subsequent days, these measurements would be made at  $60^\circ$ ,  $50^\circ$ ,  $40^\circ$ ,  $70^\circ$ ,  $60^\circ$ , . . . , and so on. Counting at the lower angles was discontinued when sufficient accuracy had been attained.



With the electron source, the count rate in the  $10^\circ$ , foil out position was initially so high that an appreciable fraction of counts was lost due to the dead time of the counter. The count rate in the  $40^\circ$ , foil in position was used instead to monitor the decay of the source. One-hour counts in the foil out and foil in positions were taken at each angle, and the angles taken in turn as previously. The count rate in the  $10^\circ$ , foil out position was taken daily, and its initial value calculated in the following way.

Let  $R(t)$  be the count rate at time  $t$ , then

$$R(t) = R(0)e^{-\lambda t}(1 - R(0)e^{-\lambda\tau}),$$

where  $\tau$  is the dead time of the counter and  $\lambda$  is known from other measurements on the decay of the source.

Then

$$\begin{aligned}\ln R(t) &= \ln R(0) - \lambda t + \ln(1 - R(0)e^{-\lambda\tau}) \\ &\simeq \ln R(0) - \lambda t - R(0)e^{-\lambda\tau} \quad (\text{since } \tau \text{ is small}),\end{aligned}$$

and

$$\frac{d}{dt} \ln R(t) = -\lambda(1 - R(0)e^{-\lambda\tau}).$$

Thus, by plotting  $\ln R(t)$  against  $t$  and measuring the slope of the curve, the correction term  $R(0)e^{-\lambda\tau}$  could be found, and hence  $R(0)$ . The correction term was quite small, being 0.038 at  $t=20$  days.

The cosmic ray background was measured and found to be independent of angle, within the statistical errors of the measurements.

The scattered intensities at the various angles had to be determined from measurements taken over about one half-life of each source. To do this, the decay was neglected over the period of each pair of foil out and foil in counts, so that for a given angle, if  $t_i$  is the time at the change over from foil out to foil in, we have

$x_i$  = the count recorded during the standard time interval at  $t_i$  with the foil out,

$y_i$  = the corresponding count with the foil in.

Then, if  $\mu_c$  = the mean rate due to cosmic rays,

$\mu_\gamma$  = the mean initial rate due to  $\gamma$ -rays from the source, and

$\mu_e$  = the mean initial rate due to electrons scattered by the foil,

$x_i$  is Poisson distributed with mean

$$\mu_c + \mu_\gamma e^{-\lambda t_i},$$

and  $y_i$  is Poisson distributed with mean

$$\mu_c + (\mu_\gamma + \mu_e)e^{-\lambda t_i}.$$

$\lambda$  and  $\mu_c$  are known, and we want to estimate  $\mu_e$  and the variance in our estimate of  $\mu_e$ . Using a least squares method, we form the sum

$$S = \sum_i [\{x_i - \mu_c - \mu_\gamma e^{-\lambda t_i}\}^2 + \{y_i - \mu_c - (\mu_\gamma + \mu_e)e^{-\lambda t_i}\}^2],$$

and from the equations

$$\frac{\partial S}{\partial \mu_e} = 0, \quad \frac{\partial S}{\partial \mu_\gamma} = 0,$$

we obtain

$$\hat{\mu}_e = \frac{\sum (y_i - x_i) e^{-\lambda t_i}}{\sum e^{-2\lambda t_i}}$$

as our estimate of  $\mu_e$ ,

$$\mu_\gamma = \frac{\sum x_i e^{-\lambda t_i} - \mu_e \sum e^{-\lambda t_i}}{\sum e^{-2\lambda t_i}},$$

and

$$\text{var}(\hat{\mu}_e) = \frac{\sum [E(x_i) + E(y_i)] e^{-2\lambda t_i}}{(\sum e^{-2\lambda t_i})^2},$$

where

$$E(x_i) = \mu_c + \hat{\mu}_\gamma e^{-t_i},$$

and

$$E(y_i) = \mu_c + (\hat{\mu}_\gamma + \hat{\mu}_e) e^{-t_i}.$$

The minimum variance in the result should be obtained if one uses a maximum likelihood rather than a least squares technique. This was done for one case, but the difference was slight, and the simpler least squares method was used throughout.

For the electron measurements, the standard errors, defined by

$$\sigma(\hat{\mu}_e) = [\text{var}(\hat{\mu}_e)]^{1/2} / \hat{\mu}_e,$$

were all less than 1 per cent., and  $x_i$  and  $y_i$  were used instead of  $E(x_i)$  and  $E(y_i)$  in the calculation of  $\text{var}(\hat{\mu}_e)$ , in which case values of  $\hat{\mu}_\gamma$  were not required.

The results of these calculations are shown in Table 2.

#### IV. COMPARISON WITH THEORY

In order to obtain usable count rates with the positron source available, the foil used was rather thicker than originally intended. As a result, the intensities of the scattered particles contained large contributions due to multiple scattering.

The usual procedure in single scattering experiments is to make corrections for multiple scattering using a technique such as that of Chase and Cox (1940) or of Butler (1950). In our case, however, the corrections obtained in this way were so large that they could not be relied upon. What was required was a complete angular distribution, covering in particular the region of transition from multiple scattering at small angles to essentially single scattering at large angles. Further, separate distributions of this kind for electrons and positrons were needed. The only existing multiple scattering theory which produces such a complete distribution in a readily calculable form is that of Molière (1948), but his theory makes no distinction between electrons and positrons. However, it has been shown by the experiments of Groetzinger, Humphrey, and Ribe (1952) and Seliger (1952) that there is a difference in the multiple scattering of these particles.

Thus a technique was devised for producing the separate electron and positron distributions. Firstly, Molière's complete distribution  $f(\chi)^*$  was calculated up to  $\chi = 120^\circ$ , taking the effective thickness of the foil to be its actual

\* Molière (1948), equation (7.3), p. 88.

thickness divided by  $\cos 11^\circ$ . This angle of  $11^\circ$  was the mean angle that the incident particles made with the normal to the foil, as estimated from the calculated trajectories in the spectrometer. Now, for large values of  $\chi$ ,  $f(\chi)$

TABLE 2  
EXPERIMENTAL RESULTS

Positrons			
$\theta$	$\hat{\mu}_\gamma$ (counts/4 hr)	$\hat{\mu}_e$ (counts/4 hr)	$\sigma(\hat{\mu}_e)$ (%)
$40^\circ$	296.6	1448	2.45
$50^\circ$	265.2	416	5.22
$60^\circ$	167.1	168.5	7.60
$70^\circ$	146.8	45.5	14.60

Electrons		
$\theta$	$\hat{\mu}_e$ (counts/hr)	$\sigma(\hat{\mu}_e)$ (%)
$40^\circ$	62800	0.40
$45^\circ$	39600	0.55
$50^\circ$	25800	0.63
$55^\circ$	16760	0.68
$60^\circ$	11590	0.68
$65^\circ$	7570	0.81
$70^\circ$	5150	0.72

$10^\circ$ , foil out rates : 100.6/min (positrons), 15780/min (electrons).

From these figures, we calculate  $R_E(\theta)$  = ratio of electron intensity to positron intensity.

$\theta$	$R_E(\theta)$	Standard Error (%)
$40^\circ$	1.11	2.5
$50^\circ$	1.58	5.3
$60^\circ$	1.75	7.6
$70^\circ$	2.88	14.6

asymptotes as expected to the single scattering distribution from which it is generated. However, instead of the exact single scattering distribution

$$I(\chi) = x^2 \operatorname{cosec}^4 \frac{1}{2}\chi \cdot R(\chi), \quad \dots\dots\dots (1)$$

Molière uses the approximate form

$$I'(\chi) = 16\kappa^2/\chi^4.$$

For large values of  $\chi$ , this is a poor approximation, and the result is that, for electrons,  $f(\chi)$  lies well below the exact single scattering distribution at large angles, as is shown in Figure 4.

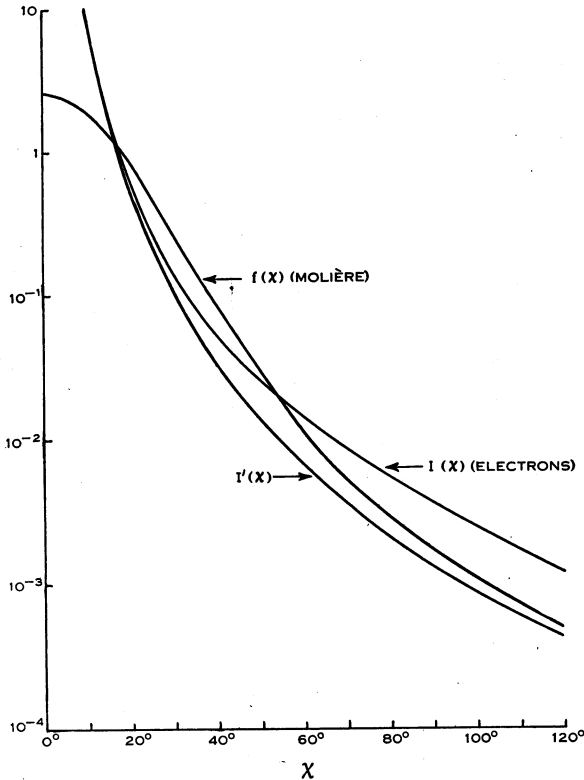


Fig. 4.—Relation between multiple and single scattering distributions.

A new distribution was then formed by calculating

$$f'(\chi) = I(\chi)[f(\chi)/I'(\chi)].$$

The implication here is that the ratio  $f(\chi)/I'(\chi)$  is regarded as giving the relation between the single scattering distribution and the multiple scattering distribution resulting from it.

Next, the function

$$y(\chi) = [f'(\chi) - f(\chi)] \cdot 2\pi \sin \chi$$

was calculated.

Now our function  $f'(\chi)$  is un-normalized. Since  $f'(\chi)$  is very small indeed for angles greater than  $120^\circ$ , we can normalize it by multiplying by  $1/k'$ , where

$$k' = \int_0^{2\pi/3} f'(\chi) \cdot 2\pi \sin \chi d\chi.$$

However, we know what values our final distribution should take for angles near  $120^\circ$ , because at these angles we find that the Chase and Cox correction for multiple scattering\* is less than 15 per cent. and therefore can be taken as giving fairly accurately the corrections to be applied to  $I(\chi)$ . Denoting the Chase and Cox correction by  $[1+C(\chi)]$ , we now have to modify slightly our function  $f'(\chi)$ , so that it becomes  $f_n(\chi)$ , with

$$\frac{1}{k}f_n(120^\circ)=I(120^\circ)[1+C(120^\circ)],$$

where

$$k=\int_0^{2\pi/3} f_n(\chi) \cdot 2\pi \sin \chi d\chi.$$

We can write

$$f'(\chi)=f(\chi)+y(\chi)/2\pi \sin \chi,$$

and so the modification can be made by replacing  $y(\chi)$  by a new function  $y_n(\chi)$ , such that

$$f_n(\chi)=f(\chi)+y_n(\chi)/2\pi \sin \chi,$$

where

$$\frac{f(120^\circ)+y_n(120^\circ)/2\pi \sin 120^\circ}{\int_0^{2\pi/3} f(\chi) \cdot 2\pi \sin \chi d\chi + \int_0^{2\pi/3} y_n(\chi) d\chi} = I(120^\circ)[1+C(120^\circ)]. \dots (2)$$

A slightly different technique for choosing  $y_n(\chi)$  was adopted for the cases of electrons and of positrons. In the electron case,  $y(\chi)$  was found to be well fitted throughout the range by a function of the form

$$y(\chi)=a(1-e^{-b\chi^2})e^{-c\chi}.$$

Then the parameters  $a$ ,  $b$ , and  $c$  were varied by trial until condition (2) was satisfied. For the positron case, it was found that plotting  $\log y(\chi)$  against  $\chi$  gave practically a straight line from  $\chi=60^\circ$  onwards. Suitable values of  $y_n(\chi)$  were obtained by replacing this straight section by the tangent to the curve at an angle slightly less than  $60^\circ$ .

The whole calculation was designed to produce distribution curves which only differed slightly from the general form of the Molière distribution, and the final normalized distributions are shown in Figures 5 (a) and 5 (b).

The justification for the somewhat arbitrary procedure adopted is that the resultant distributions have the following features:

(1) In the multiple scattering region, they have very much the same form as that of Molière, and in fact differ from the latter by 10 per cent. or less for angles up to  $35^\circ$ . This similarity in form is regarded as desirable, in view of the recent measurements of Hanson *et al.* (1951), who obtain good agreement with

\* The second order correction

$$\frac{\Delta I(\chi)}{I(\chi)} = \epsilon^2 (\operatorname{cosec}^2 \frac{1}{2}\chi - \frac{1}{2}) + \epsilon^4 \left( \frac{9}{16} \operatorname{cosec}^4 \frac{1}{2}\chi - \frac{11}{24} \operatorname{cosec}^2 \frac{1}{2}\chi + \frac{1}{24} \right)$$

has been used here. This expression was derived by Lipkin (1950), but with some numerical errors in the coefficients.

Molière's distribution for a case in which the mean angle of the distribution is of the order of  $3^\circ$ , i.e. the approximate single scattering cross section can be regarded as valid.

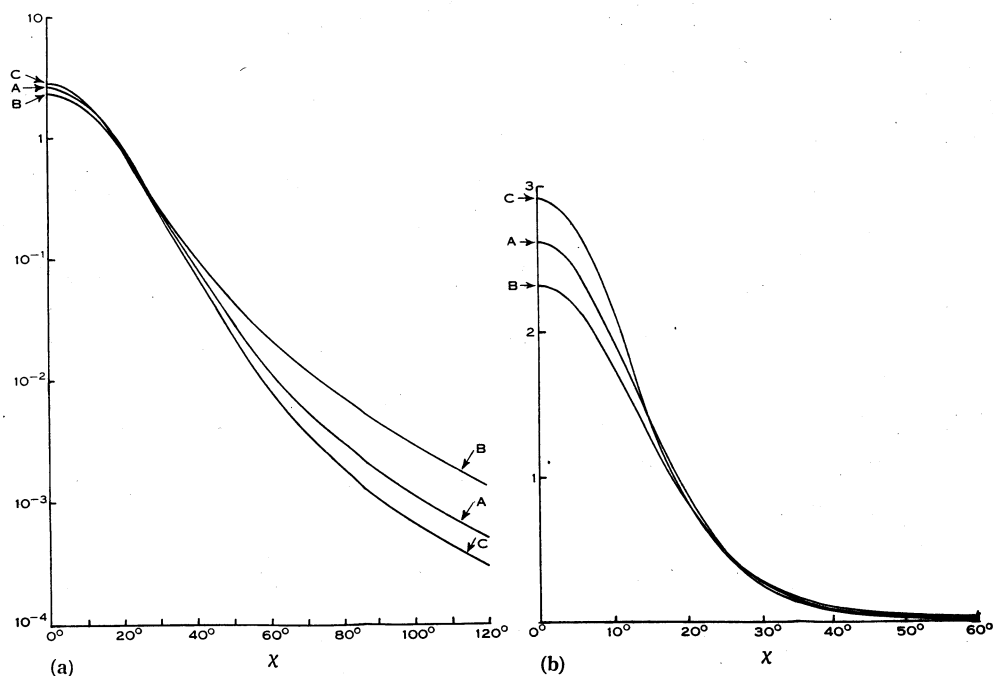


Fig. 5.—Normalized complete angular distributions shown on logarithmic (a) and linear (b). Curve A, original Molière distribution,  $f(\chi)$ ; curve B,  $(1/k)f_n(\chi)$  for electrons; curve C,  $(1/k)f_n(\chi)$  for positrons.

(2) At large angles, the distributions take the values predicted by the accurate single scattering theory, corrected for the effect of multiple scattering. It is shown in Table 3 that, while the distributions were obtained by forcing a fit at  $120^\circ$ , the agreement is good over a considerable angular range.

TABLE 3  
COMPARISON OF VALUES OF THE CORRECTED SINGLE SCATTERING DISTRIBUTIONS WITH THE VALUES OF OUR FINAL DISTRIBUTIONS

$\chi$	Electrons		Positrons	
	$\frac{1}{k}f_n(\chi)$	$I(\chi)[1+C(\chi)]$	$\frac{1}{k}f_n(\chi)$	$I(\chi)[1+C(\chi)]$
$90^\circ$	0.00466	0.00465	0.001090	0.001083
$100^\circ$	0.00299	0.00296	0.000670	0.000663
$110^\circ$	0.00199	0.00196	0.000440	0.000440
$120^\circ$	0.00134	0.00134	0.000300	0.000300

(3) The mean angles of the distributions are  $22.9^\circ$  for electrons and  $19.0^\circ$  for positrons, a difference which is consistent with the experimental results which compare the multiple scattering of electrons and positrons. Groetzinger, Humphrey, and Ribe (1952) report an r.m.s. angle for positrons 10 per cent. less than that for electrons scattered in nitrogen. Lasich (1948) obtained a smaller mean angle for positrons than for electrons with gold as the scatterer, although his results are hardly significant in this respect.

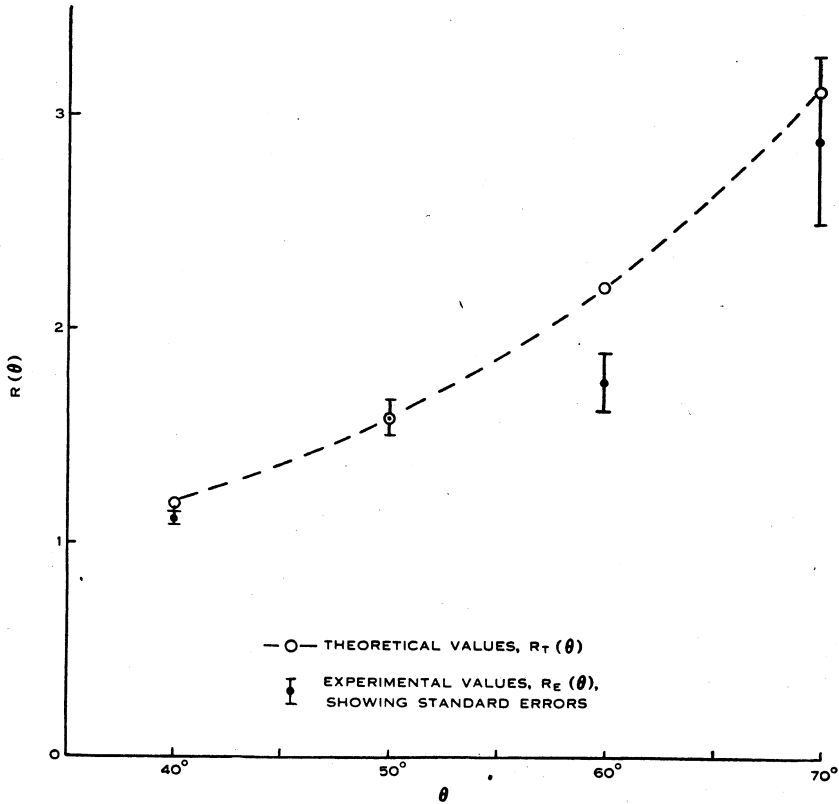


Fig. 6.—Values of the electron-positron ratio.

Finally, to calculate the expected scattered intensities in our apparatus, the incident beam was regarded as being uniformly distributed round the surface of a cone of half-angle  $\alpha$ , in which case, the fraction of the beam scattered into an element of solid angle  $d\Omega$  at an angle  $\theta$  in the apparatus is

$$P(\theta)d\Omega = \frac{d\Omega}{2\pi} \int_0^{2\pi} \frac{1}{k} f_n(\chi) d\varphi,$$

where  $\cos \chi = \cos \alpha \cos \theta + \sin \alpha \sin \theta \cos \varphi$ .

All the integrations in the above work were, of course, carried out numerically.

For comparison with the experimental results, we calculate

$$R_T(\theta) = P(\theta) - P(\theta)^+,$$

the superscripts referring to electrons and positrons. These are compared with the values  $R_E(\theta)$  from Table 2, in Figure 6.

Also the ratios  $\rho(\theta) = \hat{\mu}_e(\theta)/P(\theta)$  were calculated for electrons and positrons, and these are shown in Figure 6.

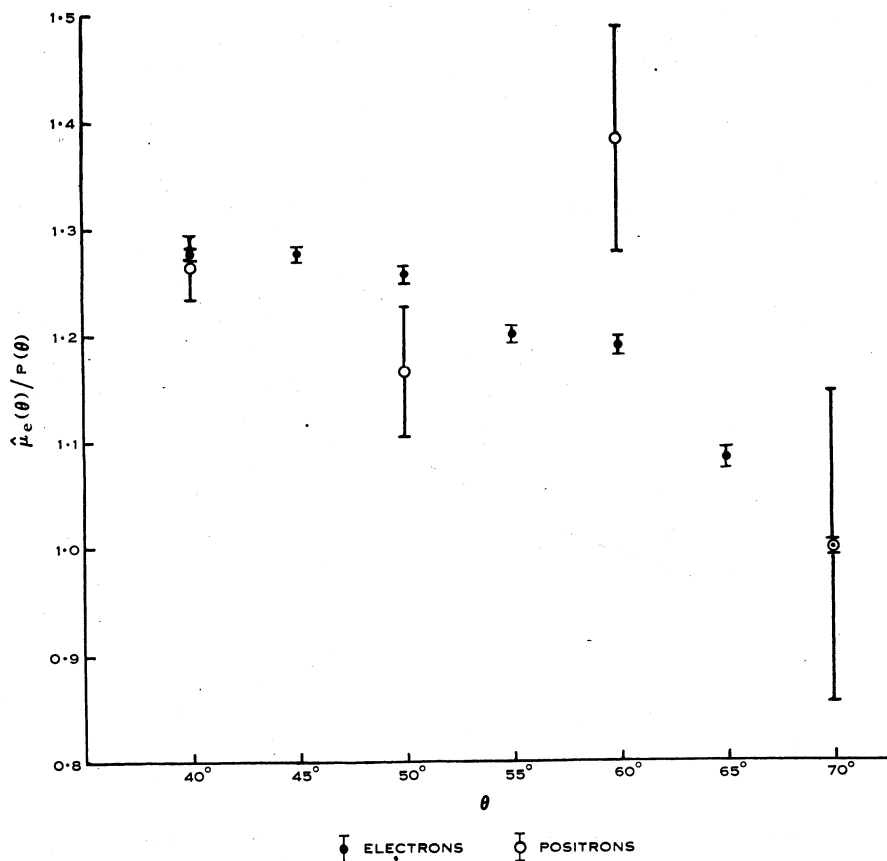


Fig. 7.—Ratios of experimental and theoretical intensities. The ratios have been multiplied by the appropriate factors to reduce the 70° value to unity in each case.

## V. DISCUSSION

The experimental results clearly establish a variation of the electron-positron ratio with the angle of scattering. Whether or not the measured values of the ratio can be said to agree with the theoretical values, depends on how much reliance can be placed on the calculations outlined in Section IV. From Figure 7, one deduces that, over this angular range, our method of calculation may have produced incorrect predicted intensities. However, since the errors introduced are, within the limits of experimental error, the same fraction of the intensity for both electrons and positrons at any angle, the electron-positron ratios as calculated will be unaltered by such errors.



If we take this to be the case, and it seems reasonable to do so, then our experimental values of the electron-positron ratio agree well with theory, and confirm Gunnensen's (1952) calculation which predicts no significant effect on the cross section due to the screening of the nucleus.

Also, since the mean angles of the complete angular distributions are approximately  $20^\circ$ , the existence of an electron-positron ratio for angles of the order of twice the mean leads to the conclusion that electrons and positrons must have different multiple scattering distributions. This is not predicted by any of the existing theories of multiple scattering.

## VI. ACKNOWLEDGMENTS

I have to thank Professor L. H. Martin and Associate Professor C. B. O. Mohr for many valuable discussions and their continued interest. Thanks are also due to Mr. E. M. Gunnensen for assistance with the experimental work, and Dr. G. Watson for advice concerning the analysis of the measurements.

## VII. REFERENCES

- BARTLETT, J. H., JR., and WATSON, R. E. (1940).—*Proc. Amer. Acad. Arts Sci.* **74**: 53.  
 BUECHNER, W. W., VAN DE GRAAF, R. J., SPERDUTO, A., BURRILL, E. A., and FESHBACH, H. (1947).—*Phys. Rev.* **72**: 678.  
 BUTLER, S. T. (1950).—*Proc. Phys. Soc. Lond. A* **63**: 599.  
 CHASE, C. T., and COX, R. T. (1940).—*Phys. Rev.* **58**: 243.  
 CHENG, L. S., DICK, J. L., and KURBATOV, J. D. (1952).—*Phys. Rev.* **88**: 887.  
 CUSACK, N. (1952).—*Phil. Mag.* **43**: 671.  
 DEUTSCH, M., ELLIOTT, L. G., and EVANS, R. D. (1944).—*Rev. Sci. Instrum.* **15**: 178.  
 FOWLER, W. A., and OPPENHEIMER, J. (1938).—*Phys. Rev.* **54**: 320.  
 GROETZINGER, G., HUMPHREY, W., JR., and RIBE, F. L. (1952).—*Phys. Rev.* **85**: 78.  
 GUNNENSEN, E. M. (1952).—*Aust. J. Sci. Res. A* **5**: 258.  
 HANSON, A. O., LANZL, L. H., LYMAN, E. M., and SCOTT, M. B. (1951).—*Phys. Rev.* **84**: 634.  
 HOWATSON, A. F., and ATKINSON, J. R. (1951).—*Phil. Mag.* **42**: 1186.  
 LANDAU, L. (1944).—*J. Phys. Moscow* **8**: 201.  
 LASICH, W. B. (1948).—*Aust. J. Sci. Res. A* **1**: 249.  
 LIND, D. A., BROWN, J. R., and DU MOND, J. W. (1949).—*Phys. Rev.* **76**: 1838.  
 LIPKIN, H. J. (1950).—Ph.D. Thesis, Princeton University.  
 LIPKIN, H. J. (1952).—*Phys. Rev.* **85**: 517.  
 MCKINLEY, W. A., JR., and FESHBACH, H. (1948).—*Phys. Rev.* **74**: 1759.  
 MASSEY, H. S. W. (1942).—*Proc. Roy. Soc. A* **181**: 14.  
 MOLIÈRE, G. (1948).—*Z. Naturf.* **3a**: 78.  
 MOTT, N. F. (1929).—*Proc. Roy. Soc. A* **124**: 425.  
 SCHULZE-PILLOT, G., and BOTHE, W. (1950).—*Z. Naturf.* **5a**: 440.  
 SELIGER, H. H. (1952).—*Phys. Rev.* **88**: 408.  
 VAN DE GRAAFF, R. J., BUECHNER, W. W., and FESHBACH, H. (1946).—*Phys. Rev.* **69**: 452.